

## The influence of ferric oxide on the properties of $3\text{CaO} \cdot 3\text{Al}_2\text{O}_3 \cdot \text{CaSO}_4$ <sup>1</sup>

Dun Chen<sup>a</sup>, Xiuji Feng<sup>b</sup> and Shizhong Long<sup>b</sup>

<sup>a</sup> *Dept. of Chemistry, The University of Toledo, OH 43606 (USA)*

<sup>b</sup> *Dept. of Materials Sciences, The Wuhan University of Technology, Hubei 430070 (People's Republic of China)*

(Received 11 May 1992)

### Abstract

It was determined that at 22.31 wt.%,  $\text{Fe}_2\text{O}_3$  reached a maximum solid solution in  $3\text{CaO} \cdot 3\text{Al}_2\text{O}_3 \cdot \text{CaSO}_4$  by replacing  $\text{Al}_2\text{O}_3$ . The physical properties of the compound with and without  $\text{Fe}_2\text{O}_3$  were measured and these are combined with the analysis of the hydration process and products by using XRD, DTA and calorimeter equipment to determine the heat of hydration etc. The results show that there was no tricalcium aluminate hexahydrate ( $3\text{CaO} \cdot \text{Al}_2\text{O}_3 \cdot 6\text{H}_2\text{O}$ ) formed in any of the samples. The addition of  $\text{Fe}_2\text{O}_3$  into the  $3\text{CaO} \cdot 3\text{Al}_2\text{O}_3 \cdot \text{CaSO}_4$  caused an initial decrease in the early compressive strength but not much in the final strength. Further, the sample with  $\text{Fe}_2\text{O}_3$  has a lower hydration heat.

### INTRODUCTION

The compound  $3\text{CaO} \cdot 3\text{Al}_2\text{O}_3 \cdot \text{CaSO}_4$  was found and identified in a study of the  $\text{CaO}-\text{Al}_2\text{O}_3-\text{CaSO}_4$  system in the 1960s [1]. Because this compound has the property of expansion after it hydrates, it became very important in the cement industry by offering the possibility of compensating for a disadvantage of cements, namely shrinkage after hardening, which can cause fracture of fabricated components. It thus became the main component of expansive cements. Because the properties should be related to the structure of the compound, the structure of  $3\text{CaO} \cdot 3\text{Al}_2\text{O}_3 \cdot \text{CaSO}_4$  was studied [2] by producing a single crystal. From this structure, it was evident that the big "hole" in the unit cell is the reason of the very high reactivity.

In order to explore the possibility of producing a new kind of cement,  $\text{Fe}_2\text{O}_3$  was added to  $3\text{CaO} \cdot 3\text{Al}_2\text{O}_3 \cdot \text{CaSO}_4$  with the expectation that it

---

*Correspondence to:* D. Chen, Dept. of Chemistry, The University of Toledo, OH 43606, USA.

<sup>1</sup> Cement chemists' notation: C = CaO; A =  $\text{Al}_2\text{O}_3$ ; F =  $\text{Fe}_2\text{O}_3$ ; H =  $\text{H}_2\text{O}$ .

would decrease the manufacturing temperature and increase the ability to withstand grinding. The properties of this series of compounds (CF system) are reported in this study. The maximum percentage of the replacement of aluminum oxide by ferric oxide was studied. Further, by following the process of hydration more information was obtained and this helped explain the properties of this series of compounds.

## EXPERIMENTAL

### Materials

Various ratios of analytical reagents, calcium carbonate ( $\text{CaCO}_3$ ), aluminum oxide ( $\text{Al}_2\text{O}_3$ ), calcium sulfate ( $\text{CaSO}_4 \cdot 2\text{H}_2\text{O}$ ) and ferric oxide ( $\text{Fe}_2\text{O}_3$ ) were used to obtain appropriate mixtures calculated from the formula  $3\text{CaCO}_3 \cdot (3-x)\text{Al}_2\text{O}_3 \cdot x\text{Fe}_2\text{O}_3 \cdot \text{CaSO}_4 \cdot 2\text{H}_2\text{O}$ , where  $x = 0, 0.2, 0.4, 0.6, 0.8, 1.0, 1.2$  and  $1.4$ . The symbols and compositions of samples are shown in Table 1. The samples were ground and mixed thoroughly, the appropriate amount of water was added to form a compact about 10 mm thick and 20 mm in diameter under pressure. After sintering each sample in the form of a wet compact at a temperature of 1100–1350°C for 3 hours, it was cooled in air and ground again to obtain the final product, which was stored in a desiccator.

The compressive strength of each sample was measured by using neat paste in a small mould ( $2 \times 2 \times 2 \text{ cm}^3$ ) and a water/solid ratio (w/c) of 0.29. In order to investigate the possibility of producing a new kind of cement, calcium aluminate ( $\text{CaO} \cdot \text{Al}_2\text{O}_3$ ) and calcium dialuminate ( $\text{CaO} \cdot 2\text{Al}_2\text{O}_3$ ) were prepared by mixing  $\text{CaCO}_3$  and  $\text{Al}_2\text{O}_3$  thoroughly grinding, moulding to form wet compacts which were sintered at 1400°C for 4 h, cooling in air and finally grinding to obtain the products. They were added to the  $3\text{CaO} \cdot 3\text{Al}_2\text{O}_3 \cdot \text{CaSO}_4$ . The two materials were mixed in the ratio 50 wt.%. These two samples were called CA and CA2,

TABLE 1

Compositions of the samples (wt.%)

Sample	$\text{CaCO}_3$	$\text{Al}_2\text{O}_3$	$\text{CaSO}_4 \cdot 2\text{H}_2\text{O}$	$\text{Fe}_2\text{O}_3$
CF00	38.58	39.30	22.12	
CF02	38.02	36.14	21.80	4.04
CF04	37.47	33.08	21.48	7.97
CF06	36.94	30.10	21.18	11.79
CF08	36.42	27.20	20.88	15.50
CF10	35.92	24.39	20.59	19.10
CF12	35.43	21.65	20.31	22.61
CF14	34.95	18.99	20.04	26.02

corresponding to the added  $\text{CaO} \cdot \text{Al}_2\text{O}_3$  and  $\text{CaO} \cdot 2\text{Al}_2\text{O}_3$  respectively. The samples were mixed with water (w/c ratio 0.29), cured for one day in a humidity chamber and cured in water at 25°C. At 3, 7 and 28 days the compressive strengths were measured.

SEM pictures were taken of some samples. The samples were immediately immersed in ethanol (AR grade) to obtain the micrographs. To obtain more information on the hydration products, residues were ground with ethanol to a 180-mesh sieve, washed once with ethanol and then twice with acetone, heated under vacuum at 50–60°C for 2–3 h, then heated at 60°C for 3 h. The products were stored in a desiccator.

All the surface area measurements were made by using the Blain permeability apparatus.

### *Apparatus*

#### *XRD*

After mixing the sample with appropriate amounts of  $\alpha\text{-Al}_2\text{O}_3$  powder, a thin layer was exposed using the HZG4-PC X-ray diffractometer to obtain the exact positions of peaks. The Bragg equation was then used to calculate the lattice constants. The parameters of the X-ray diffractometer were  $2\theta = 1/100$ , the data collection interval was 2 s.

#### *Microcalorimeter*

By using the Seteram Microcalorimeter HT-1500 the liberated heat of hydration at 30°C was measured on a sample with a w/c of 10.

#### *DTA*

DTA patterns were measured on the Shanghai DTA equipment with the following parameters. The sensitivity was equal to 10 mV and the heating rate was 10°C min<sup>-1</sup>. The temperature range was from room temperature to 600°C.

#### *SEM*

The scanning electron micrographs were obtained using the JEOL ISI-SX-40 electron microscopy equipment. The acceleration voltage was 20 kV.

## RESULTS AND DISCUSSION

### *The maximum solid solution*

As the amount of  $\text{Fe}_2\text{O}_3$  in the CF system (see Table 1) compounds increased, the XRD peaks moved to a lower angle, which meant that the lattice constant increased. When the iron atoms in  $3\text{CaO} \cdot 3\text{Al}_2\text{O}_3 \cdot \text{CaSO}_4$

TABLE 2

Lattice constants  $a$  (Å) of the CF system

CF00	CF06	CF08	CF10	CF12	CF14
18.3832	18.4134	18.4160	18.4174	18.4194	18.4199

reached a maximum, the lattice constant of  $3\text{CaO} \cdot 3\text{Al}_2\text{O}_3 \cdot \text{CaSO}_4$  with iron atoms reached a constant value, which did not change even though there were larger amounts of iron atoms in the mixture. The results of the lattice constant determinations are shown in the Table 2 and Fig. 1; they indicate that in sample CF12 the amount of iron atoms in the compound has reached a maximum; in other words, it is saturated with iron. However, from the results of XRD on the CF system compounds shown in Table 3, it is seen that not all of the  $\text{Fe}_2\text{O}_3$  added stayed in the lattice of the compound; instead it always formed  $\text{C}_x\text{AF}_{1-x}$  (mainly in  $\text{C}_2\text{F}$  form) with CA or  $\text{C}_3\text{A}$ .

Although we know the conditions at which the maximum solid solution amount of  $\text{Fe}_2\text{O}_3$  in the compound is reached, the exact positioning of the iron atoms in the compound still poses a problem. There are two types of replacement in the crystal lattice. In the first type, the atoms of the lattice are directly replaced (Schottky defects). This kind of replacement makes the foreign atoms take part in the formation of the lattice. In the other type of defect, the minor atoms stay between the atoms of the lattice and do not take part in the formation of lattice (Frenkel defects). The latter is also a kind of bulk effect. The results of XRD show that there is always  $\text{C}_x\text{AF}_{1-x}$  (mainly in  $\text{C}_2\text{F}$  form) formed in the mixture, so we can say that there is always some  $\text{Fe}_2\text{O}_3$  left behind, while some has reacted with the compound to form the first type of replacement, owing to the small

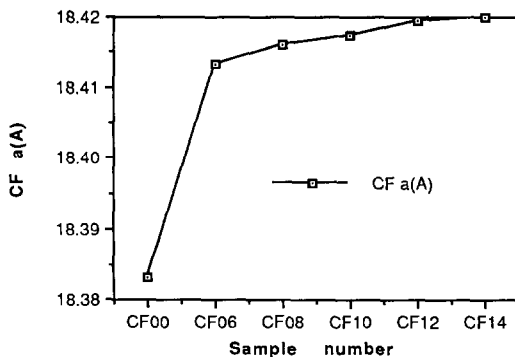


Fig. 1. The lattice constants of CF system compounds.

TABLE 3  
XRD results of CF system compounds<sup>a</sup>

Sample	3CaO · 3Al <sub>2</sub> O <sub>3</sub> · CaSO <sub>4</sub>	C <sub>x</sub> AF <sub>1-x</sub> <sup>b</sup>	CA and C <sub>3</sub> A
CF02	+ + + + +	n	+
CF02	+ + + + +	n	+
CF04	+ + + + +	T	T
CF06	+ + + +	+	T
CF08	+ + + +	+	T
CF10	+ + + +	+	n
CF12	+ + + +	+ +	n
CF14	+ + + +	+ +	n

<sup>a</sup> T, trace amount; n, does not exist; the more +, the larger the relative amount of that component.

<sup>b</sup> Mainly in the form of C<sub>2</sub>F.

difference between the radius of Fe<sup>3+</sup> (0.57 Å) and Al<sup>3+</sup> (0.47 Å). Therefore, the second type of replacement dominates.

### Strength and the process of hydration

#### Strength of the compacts

Table 4 gives the compressive strengths of the CF system compounds and the CA and CA2 samples (see the Experimental section for the composition) and Figs. 2 and 3 show the plots of strength vs. time of aging. From the data, the early strengths of the compounds with Fe<sub>2</sub>O<sub>3</sub> are lower than that of the pure compound CF00. However, the later strengths catch up with that of the pure compound. Further, when CA and CA<sub>2</sub> are added to the pure compounds corresponding to CA and CA<sub>2</sub> samples respectively, the early and later strengths of the CA<sub>2</sub> sample are higher than that of the pure compound, whereas the early strength of the CA sample is the higher but the later strength is the lower. The reason for this

TABLE 4  
Compressive strengths of CF system compounds

Sample	Surface area (cm <sup>2</sup> g <sup>-1</sup> )	Comp. strength (kg cm <sup>-2</sup> )		
		3 Days	7 Days	28 Days
CF00	3074	204	272	288
CF04	2986	198	257	269
CF08	3124	205	263	295
CA	2930	242	262	270
CA <sub>2</sub>	3070	210	284	325

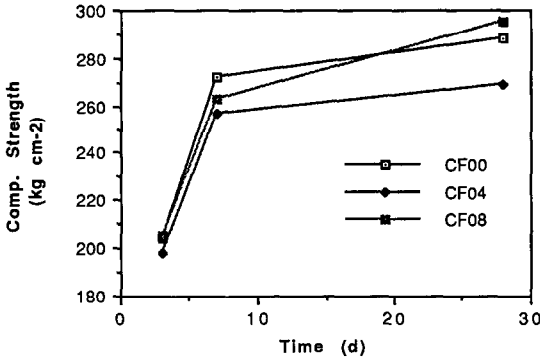


Fig. 2. Compressive strengths of CF00, CF04 and CF08.

is that the component CA in the CA sample hydrates much faster than the CA<sub>2</sub> in the CA2 sample. This causes the high porosity of the paste and lowers the final strength, but increases the early strength due to the fast hydration. In order to give some explanation of the growth of the strengths of samples, a study of their hydration is necessary.

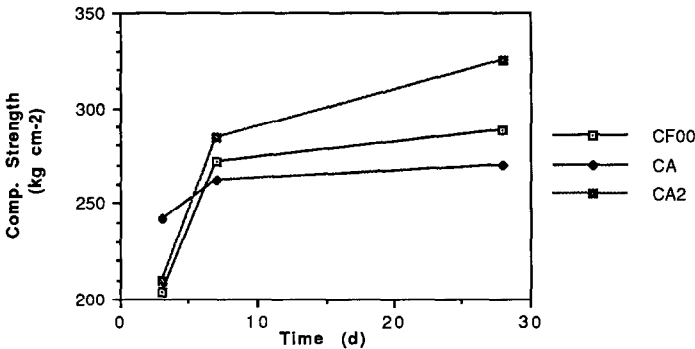


Fig. 3. Compressive strengths of CF00, CA and CA2.

### *The hydration process*

Figures 4 and 5 show the hydration heat curves of CF00 and CF06 and trends for the integration of the heat of hydration respectively. In Fig. 4, the obvious difference in the hydration curves shows that there is no induction period in the CF00 sample and the heat evolved by CF00 is much higher than by CF04. The reason for this can be accounted for by the presence of other oxide species in the CF04 sample. The other oxide species include CA, C<sub>3</sub>A and C<sub>x</sub>AF<sub>1-x</sub>. The presence of other oxide species causes the slowing down of the hydration process and causes the induction period. The lower value of the total hydration heat may also be

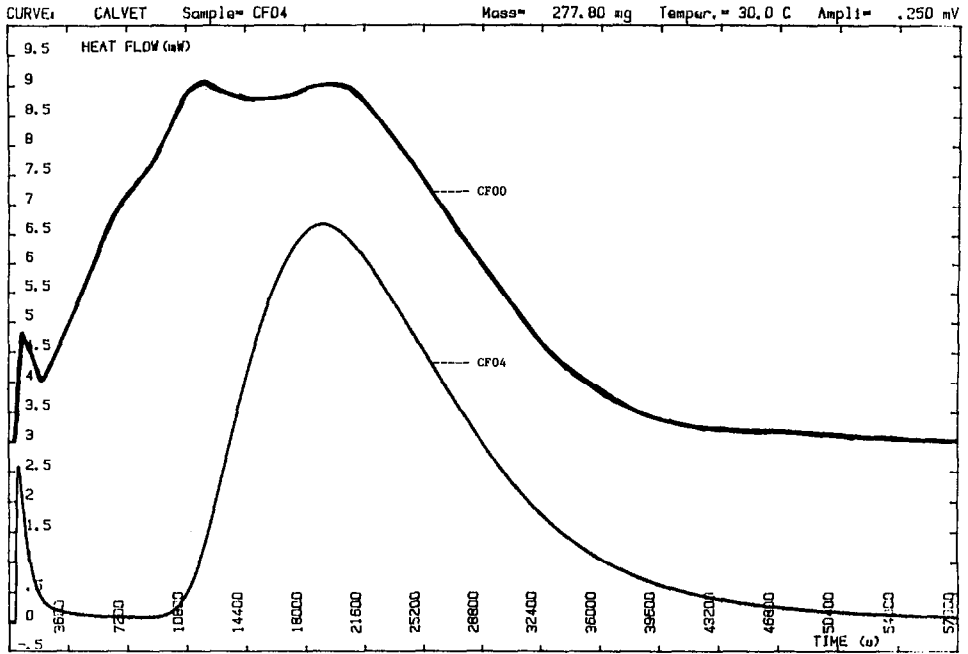


Fig. 4. The hydration curves of CF00 and CF04 samples.

due to the  $\text{Fe}_2\text{O}_3$  used in the preparation process filling the “hole” present in the structure of  $3\text{CaO} \cdot 3\text{Al}_2\text{O}_3 \cdot \text{CaSO}_4$ .

The hydration products of various samples (at various curing times) determined by XRD are shown in Table 5. Figures 6, 7 and 8 show the DTA patterns of selected samples. From these results and previous research [1, 2], the process of the hydration can then be postulated as follows.

When water is added to the sample, the main component

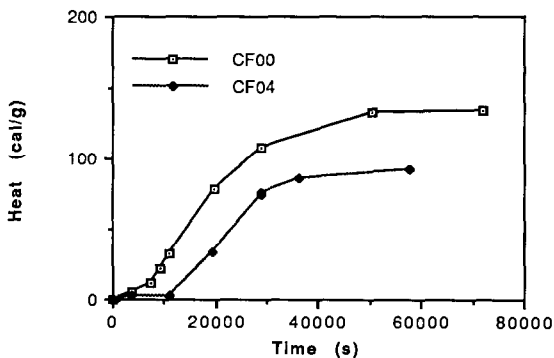


Fig. 5. The integrated hydration heats from the hydration heat curves.

TABLE 5  
XRD results of the hydration products<sup>a</sup>

Sample	Days	Unreacted	AFt <sup>b</sup>	AFm <sup>c</sup>	C <sub>2</sub> AH <sub>8</sub>	AH <sub>3</sub>
CF00	3	+++++	++	T	T	++
	7	+++++	++	+	T	++
	28	+++++	+	++	+	++
CF04	3	+++++	++	+	T	+++
	7	+++++	++	++	+	+++
	28	+++++	+++	++	+	+++
CF08	3	+++++	++	+	T	+++
	7	+++	+++	++	+	+++
	28	+++	+++	++	+	+++
CA	3	+++++	+	T	T	++
	7	+++++	+	T	T	+++
	28	+++	++	+	T	+++
CA2	3	+++++	+	T	T	++
	7	+++++	+	T	T	+++
	28	+++	++	+	T	+++

<sup>a</sup> T, trace amount; the more +, the larger the relative amount of that component. <sup>b</sup> This is the symbol for ettringite. <sup>c</sup> This is the symbol for the monosulfate calcium aluminate hydrate.

(3CaO · 3Al<sub>2</sub>O<sub>3</sub> · CaSO<sub>4</sub>) quickly hydrates and releases Ca<sup>2+</sup>, Al<sup>3+</sup> and SO<sub>4</sub><sup>2-</sup> ions. Ettringite (3CaO · Al<sub>2</sub>O<sub>3</sub> · 3CaSO<sub>4</sub> · 32H<sub>2</sub>O) is formed, with the formation of aluminum gel (Al(OH)<sub>3</sub> or AH<sub>3</sub>). Further, owing to the other oxide species in the sample, the monosulfate calcium aluminate hydrate (AFm) and the calcium aluminate hydrate (C<sub>2</sub>AH<sub>8</sub>) are formed.

After the concentrations of ions in the liquid reach a certain level and enough hydration products cover the surface of the sample, the hydration process arrives at an induction or dormant period. In this dormant stage the diffusion process is very slow because of the covering of the sample's surface by the hydration products and the common ion effect while the concentrations of ions are increasing. Thus the dormant stage is shown as the flat period in the hydration heat curves of the CF04 sample. However, in the CF00 sample there is a very short induction period, due to the hexagonal and needle like crystals formed in the initial hydration step being too few to cover the surface of the reactant. Further, the impurities cause the rapid increase in the concentrations in the ions in the liquid.

When the concentration of ions in the liquid reach a certain level, calcium aluminate hydrate and other hydrates crystallize again. The sudden reduction in the concentration of ions in the liquid phase and in the size of the contracting unreacted particles is due to hydration making the diffusion process faster. The hydration process then proceeds at an accelerating rate. As the hydration progresses, the rate of the hydrolysis



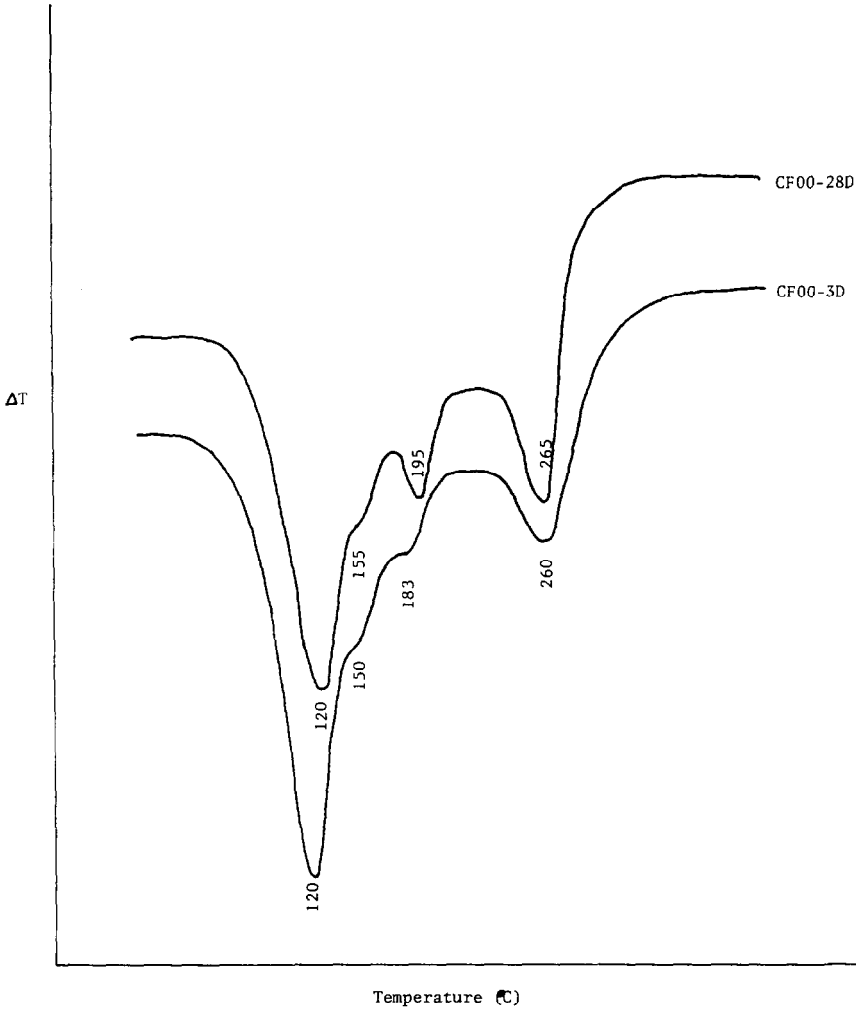


Fig. 6. The DTA curves of hydrated CF00 samples at 3 days and 28 days.

becomes faster than that of the crystal growth, which makes the concentrations of ions in the liquid phase reach another saturated level and causes the hydration process to slow down. This explanation is the reason for the appearance of the second flat period in the accelerating part of the hydration heat curves. At this time the unreacted samples become very small fragments and can react with water very easily. The hydration of these fragments is the final stage in the hydration process. This causes the final peaks in the hydration heat curves.

While  $\text{Fe}_2\text{O}_3$  is present in the sample, the initial hydrated products have greater porosity and thus cause the lower initial strengths. However, for the final strength, the process of hydration causes the pores to be filled

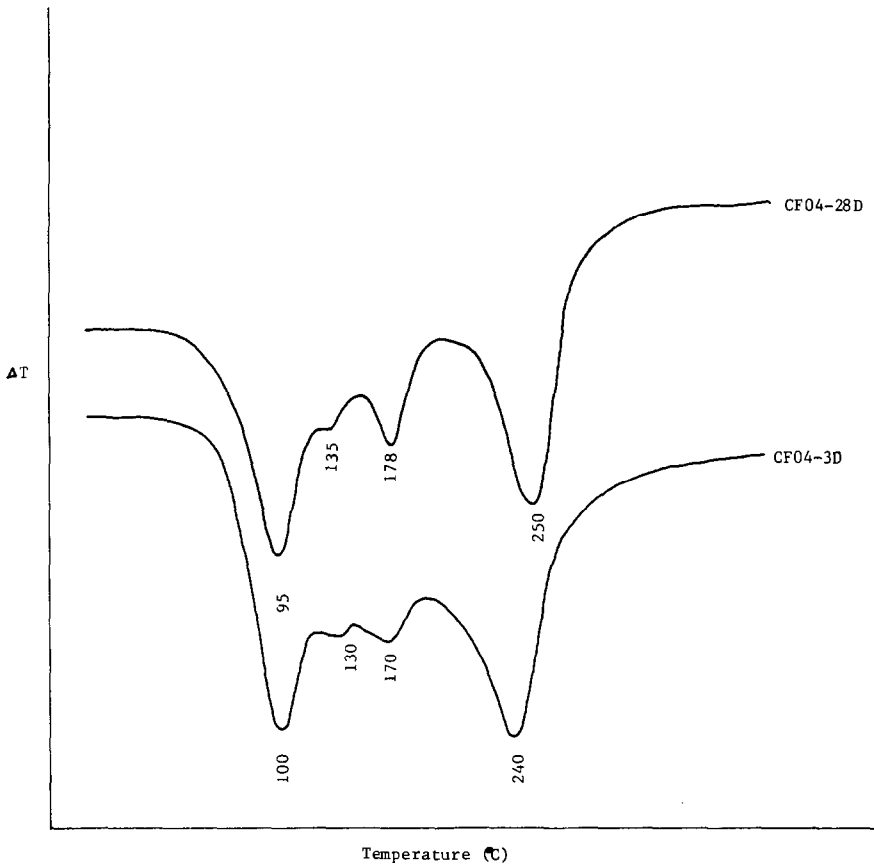


Fig. 7. The DTA curves of hydrated CF04 samples at 3 days and 28 days.

and has little effect on their final strengths. The SEM result in Figs. 9 and 10 show the difference of porosity and interaction among particles.

#### *The DTA data analysis*

In DTA patterns [3, 4], peaks around 120°C correspond to the dehydration of ettringite, peaks around 150°C correspond to the dehydration of  $C_2AH_8$ , peaks around 260°C correspond to the dehydration of  $AH_3$ , and peaks around 180°C correspond to the dehydration of AFm. From the peak temperatures and the XRD results, there was no  $C_3AH_6$  formed in any samples, especially not in the CA and CA2 samples. This property can prevent the intrinsic danger of the fracture of concrete due to the expansion caused by the transformation of calcium aluminate hydrates into cubic  $C_3AH_6$ .

When the change of the peak temperatures are taken into account, the results show that the longer the curing time, the higher the peak temperature, which can be explained by increased crystallinity. For

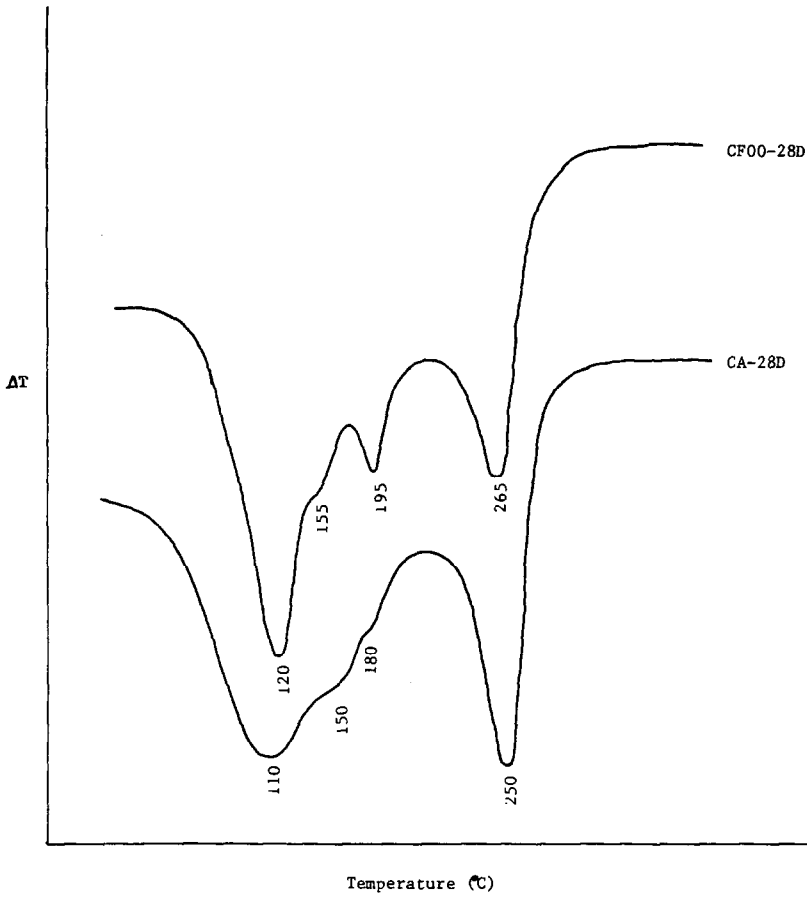


Fig. 8. The DTA curves of hydrated CF00 and CA samples at 28 days.

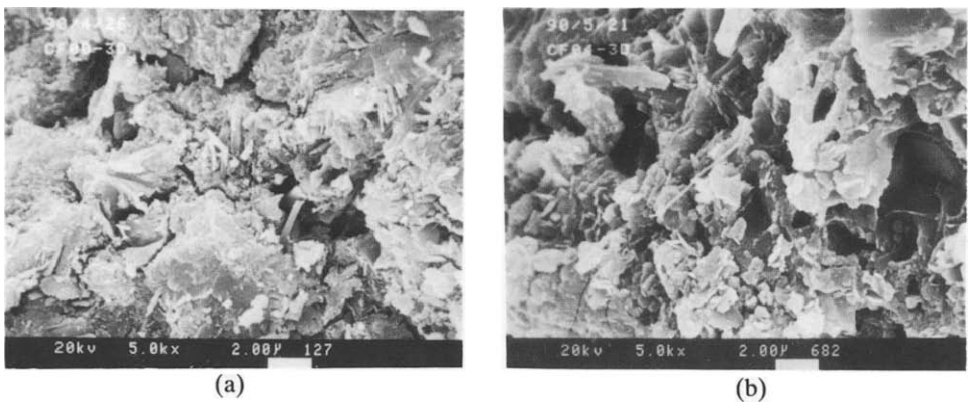


Fig. 9. Scanning electron micrograph. Original magnification 5000×: (a), hydrated CF00 sample at 3 days; (b), hydrated CF04 sample at 3 days. Note that the rod- or needle-like crystal is ettringite, the hexagonal plates are calcium aluminate hydrates (main) and AFm (minor). The porosity in (b) is much larger than that in (a), which accounts for the low compressive strength of (b) sample.

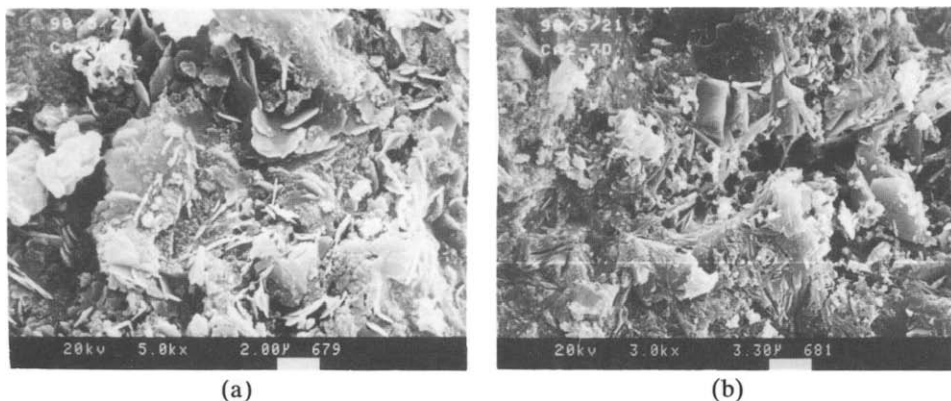


Fig. 10. Scanning electron micrograph. Original magnification 5000 $\times$ : (a), hydrated CA sample at 3 days; (b), hydrated CA2 sample at 7 days. Note that the fast hydration of CA in the CA sample and the relatively large amount of hexagonal hydrates in the CA sample (a) causes low interaction between particles. This accounts for the low final strength of the CA sample.

example, in the hydrated CF00 sample at 3 days and 28 days, the peaks around 150 $^{\circ}$ C, 180 $^{\circ}$ C and 260 $^{\circ}$ C which correspond to the dehydration of C<sub>2</sub>AH<sub>8</sub>, AFm and AH<sub>3</sub> respectively, show the trend CF00-28D > CF00-3D. However, the peak temperatures of ettringite (around 120 $^{\circ}$ C) show the opposite trend. This is due to the transformation of ettringite into the monosulfate form. This process causes the ettringite to be “dissolved” and become more disordered.

## CONCLUSIONS

(1) The condition for Fe<sub>2</sub>O<sub>3</sub> to reach the maximum solid solution in 3CaO · 3Al<sub>2</sub>O<sub>3</sub> · CaSO<sub>4</sub> is about 22.61 wt.% Fe<sub>2</sub>O<sub>3</sub> in the preparation process.

(2) The addition of Fe<sub>2</sub>O<sub>3</sub> causes a slight decrease of the early compressive strength, which is due to the formation of C<sub>x</sub>AF<sub>1-x</sub> (mainly in C<sub>2</sub>F form).

(3) The initial hydration processes of 3CaO · 3Al<sub>2</sub>O<sub>3</sub> · CaSO<sub>4</sub> is

$$3\text{CaO} \cdot 3\text{Al}_2\text{O}_3 \cdot \text{CaSO}_4 + \text{H}_2\text{O} \rightarrow \text{Ettringite (main)} \\ + \text{AH}_3 + \text{monosulfate (minor)}$$

Ettringite is slowly transformed into the monosulfate.

(4) There is no C<sub>3</sub>AH<sub>6</sub> formed (which would have caused a reduction in strength), even when CA and CA<sub>2</sub> are added to the sample. This property makes the manufacture of high early- and final-strength aluminum sulfate cements possible.

(5) The presence of Fe<sub>2</sub>O<sub>3</sub> in the preparation process causes a long induction period in the hydration process of the samples. Further, the total hydration heat is lowered.

## ACKNOWLEDGMENTS

D.C. acknowledges that all the work was performed under the guidance of Prof. Dr.-Ing. Feng, who taught him not only how to do research but also how to pursue a career in life. He was much more to D.C. than an advisor. We are also very appreciative of our colleagues, Dr. Hu Shuguang, Mr. Liao, etc., who helped us with the difficult experiments.

## REFERENCES

- 1 F.M. Lea, *The Chemistry of Cement and Concrete*, 3rd edn., Arnold, London, 1970.
- 2 L. Guangling, Thesis for Master's degree, The Wuhan University of Technology, 1986.
- 3 V.S. Ramachandran, *Application of DTA in Cement Chemistry*, Chemical Publishing Co., New York, 1969.
- 4 M. Murat, Proc. Int. Sem. on Calcium Aluminates, Turin, 1982, Polytechnico di Torino, 1982, p. 59.